# EXPERIMENTAL STUDY OF ESSENTIALLY NON-STATIONARY ACOUSTIC RECEPTIVITY OF A BOUNDARY LAYER ON AN AIRFOIL DUE TO SURFACE NON-UNIFORMITIES

**A.V. Ivanov[1], W. Würz[2], S. Herr[2], S. Wagner[2], and Y.S. Kachanov[1]**

[1] Institute of Theoretical and Applied Mechanics SB RAS,
630090 Novosibirsk, Russia

[2] Institut für Aerodynamik und Gasdynamik, Universität Stuttgart, Stuttgart, Germany

## 1. Introduction

In most cases the boundary layer transition process starts with the receptivity stage, when external perturbations are transformed into boundary layer instability waves. One of the possible mechanism of the instability wave onset is the scattering of external acoustic perturbations on aerodynamic surface non-uniformities. Considerable progress in the investigation of this process is achieved and receptivity coefficients were obtained in cases when acoustic scatters on a surface roughness. The 3D *roughness-acoustic receptivity* mechanism on a *2D airfoil*, was investigated experimentally and numerically in [1] and the receptivity coefficients were determined as functions of the frequency and the wave obliqueness. The present work is a continuation of [1] and it is devoted to the investigation of the acoustic receptivity due to localised surface vibrations (*vibration-acoustic receptivity*). As it was experimentally proved in [2] and in [1], the excitation of instability waves in a boundary layer at these conditions takes place at combination frequencies $f_w = f_{ac} \mp f_v$, where $f_{ac}$ – frequency of acoustics, $f_v$ – frequency of surface vibrations. In both noted experiments the frequencies of the applied surface vibrations were much lower than the acoustic frequency (in [1] $f_v/f_{ac}$=1/64), so the receptivity process physically corresponded to acoustic-roughness interaction. The case, when acoustic and surface vibrations have comparable frequencies has not been studied at all, despite such situation seems very realisable at flight conditions. The important peculiarity of this receptivity mechanism is that both participating frequencies ( $f_{ac}$ and $f_v$), may lie in the range of stable frequencies and *do not* produce in the boundary layer any amplified perturbations, but the resulting TS-wave may lie in the range of unstable frequencies and can provoke earlier transition. This work is intended to study systematically the vibration-acoustic mechanism of TS-wave production and to compare the obtained receptivity results with a roughness case [1].

## 2. Experimental details

***2.1. Model and flow parameters.*** The experiments were carried out in the Laminar Wind Tunnel (LWT) of the IAG. The LWT is an open return tunnel with a turbulence level less than $Tu=2\times10^{-4}$. The boundary layer measurements were performed on a symmetrical airfoil section at zero angle of attack and at a Reynolds number of $1.2\times10^6$ based on the arclength $s_{max}$ = 0.615 m measured from the leading edge. The surface vibrator was placed at streamwise coordinate $s/s_{max}$=0.2. The free stream velocity at this position was 36 m/s, the local Reynolds number based on the boundary layer displacement thickness at the position of vibrator ($\delta_{1v}$=0,356 mm) was $Re_{\delta 1}$ = 850. All model parameters, flow parameters (Re) and the frequency parameters of the instability waves under investigation were similar to [1], in order to have comparable results on the receptivity in both experiments.

***2.2. Disturbance parameters.*** For the investigation of different cases of interaction between surface vibrations and acoustic, it is convenient to introduce a parameter *K*, which

characterises the ratio of the surface vibration frequency to the acoustic one: $K = f_v/f_{ac}$. As was mentioned above, the generation of TS-waves takes place at combination frequencies $f_{TS} = f_{ac} + f_v$ ('plus-regime') and $f_{TS} = f_{ac} - f_v$ ('minus-regime'). The present paper focuses on the following plus-regimes of interaction:

*a*) $K = f_v/f_{ac} = 0.217$, $f_{ac} = 873$ Hz, $f_v = 190$ Hz, $f_{TS1} = f_{ac} + f_v = 1063$ Hz;
*b*) $K = f_v/f_{ac} = 0.434$, $f_{ac} = 742$ Hz, $f_v = 323$ Hz, $f_{TS1} = f_{ac} + f_v = 1065$ Hz;
*c*) $K = f_v/f_{ac} = 0.98$, $f_{ac} = 537$ Hz, $f_v = 526$ Hz, $f_{TS1} = f_{ac} + f_v = 1063$ Hz.

The receptivity data for a higher TS-wave frequency ($f_{TS} = f_{TS2} = 1594$ Hz) were measured in regime:

*d*) $K = f_v/f_{ac} = 0.217$, $f_{ac} = 1309$ Hz, $f_v = 285$ Hz, $f_{TS2} = f_{ac} + f_v = 1594$ Hz.

All disturbance frequencies were chosen in such a way, that the frequencies of the combination modes were close to the TS-wave frequencies investigated in [1]. Together with the data obtained in [1], *regimes a-c* should provide comparable data on the vibration-acoustic receptivity, when TS-waves of the same frequency are excited by different combinations of frequencies of the surface vibrations and acoustics. The receptivity data obtained in *regime d* are also comparable to [1] and should clarify a dependence of the vibration-acoustic receptivity on the excitation frequencies.

***2.3. Disturbance simulation.*** Two high-frequency and one low-frequency loudspeakers were used in the experiment for the acoustic field generation. The loudspeakers were placed in aerodynamically smoothed housings and installed downstream the test section. The loudspeakers were powered with amplifiers and were used separately depending on the necessary sound frequency. As was found in previous experiments, the acoustic amplitude in the test section depends strongly on the environmental air temperature (via the acoustic wave length change and a transformation of the whole sound field structure inside the wind tunnel). The latter point forces to perform a control of the acoustic amplitude during the receptivity measurements. Such control was arranged with the help of a special hot-wire probe (see also section 2.4). During the receptivity measurements the typical r.m.s. values of the free-stream acoustic-velocity fluctuations above the vibrator were about 0.006÷0.01 m/s.

To simulate the localised surface vibrations, a vibrator with a vinyl circular membrane (of 6-mm diameter) was used. It was mounted into the model flush with its surface. The membrane was driven by harmonic pressure pulsations. The spatial shape of the membrane oscillations was measured thoroughly with the help of a laser triangulation vibrometer, in order to get the necessary information about the spectral content of the surface non-uniformity. In addition, a fibre-optic displacement sensor Philtec-D12 was used. This sensor was installed inside the model in a way to direct its tip on the inner surface of the vibrator membrane. The electrical output of the device, proportional to the distance from the membrane, allowed to provide a permanent monitoring of the membrane oscillations during the receptivity measurements.

***2.4. Data acquisition and measurement procedure.*** The complete experimental setup is sketched in Fig. 1. For the hot-wire measurements a probe (1 mm wire length) was used together with a DISA55M10 bridge. The second hot-wire was applied for acoustic measurements and was used in couple with an additional DISA55M10 bridge. Two PCs were used in the experiment. The first one controled the traverse and the data acquisition and sequencing. The second one was used for the signals' generation. The vibrational and acoustical frequencies, as well as the digital sampling trigger, were strictly phased locked and generated by an AD-converter of this PC. The acoustical, vibrational, and combination frequencies had integer number of periods in one sampling, that allowed to represent each of them with a single Fourier series coefficients after one FFT and enabled online control of the whole frequency spectra. The

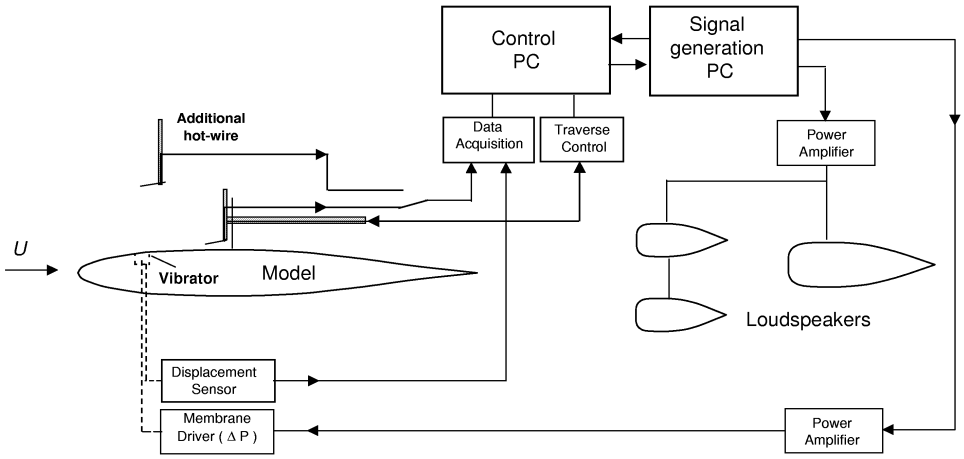


Fig. 1. Scheme of experimental setup.

data acquisition is started with a fixed phase relation to the signal for the vibrator, which played a role of a reference signal. Five sets of 4096 points were collected and ensemble averaged in the time domain before the Fourier transform. In every point of measurements, the resulting time-trace of hot-wire signal and the frequency spectra were stored on the PC hard disc. Exactly in the same way, the output of the displacement sensor Philtec D12 had been taken for each point of measurements for the control of membrane oscillations.

In the boundary layer the hot-wire measurements were performed downstream the vibrator (in its 'fare-field'), where only eigen boundary layer oscillations (the TS-instability modes) were present. In every regime of measurements, normally 4 to 5 spanwise scans (consisted of 40 to 60 spatial points each) were documented and gave the necessary information about the spatial development of disturbances. In every scan the hot-wire was positioned at the fixed non-dimensional distance to the wing surface ($y/\delta_2 = 2.2$) corresponding approximately to amplitude maxima of all studied 3D TS-modes.

The readings of the acoustic intensity with the help of the second hot-wire were done immediately before and after every spanwise scan. During these measurements the second hot-wire was included into the measurement circuit, instead of the main one, and moved to the vibrator position for the sound measurements (3 to 6 samples). After finishing the sound measurement the second hot-wire was removed from the model. Additionally, in every set of measurements two or three normal-to-wall profiles were taken, including a *y*-profile at the vibrator position ($s = 123$ mm, $z = 0$).

### 3. Direct results of boundary layer measurements

A typical frequency spectrum of the hot-wire signal, observed in the boundary layer downstream the vibrator ($s = 150$ mm) in presence of the acoustic field, is shown in Fig. 2 (the amplitudes are shown in logarithmic scale). The frequencies of vibrations and acoustics here are: $f_v = 190$ and $f_{ac} = 873$ Hz (*regime a)*. The spectral components at these frequencies have, as expected, the highest amplitudes in the boundary layer. Thus, the localised surface vibration with the amplitude of about 10% of $\delta_1$ (~35μm in the vibrator center) provides excitation in the boundary layer of local velocity fluctuations of about 1%. The signal at the acoustic frequency is also very intensive and consists mainly of a mixture of: (*i*) the acoustic field itself, including the Stokes layer in the near-wall region;

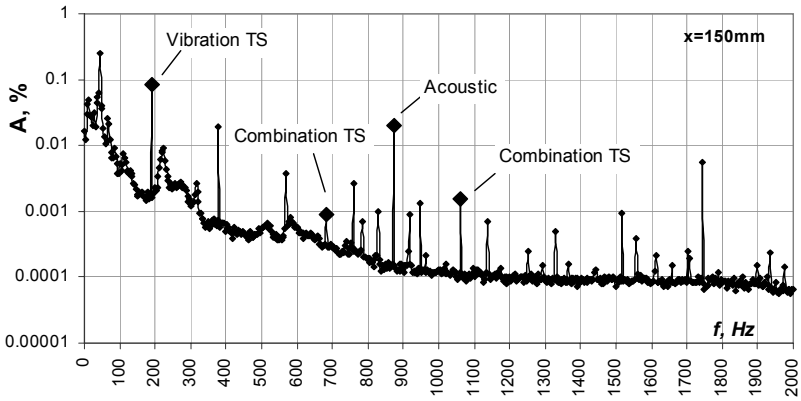


Fig. 2. Typical frequency spectrum of hot-wire signal measured in boundary layer. Regime *a*.

(*ii*) the vibrations of the hot-wire probe and the model surface, and (*iii*) the instability waves generated by the acoustics. The results of the interaction of the surface vibrations and the acoustics take place at the combination frequencies, here at: $f_{TS} = f_{ac} - f_v = 683$ Hz (minus-regime) and $f_{TS} = f_{ac} + f_v = 1063$ Hz (plus-regime). In this case the combination frequency under investigation ($f_{TS1} = 1063$ Hz) is one of the most unstable, and the disturbances of this frequency are amplified downstream. Spatial development of these perturbations shown in Fig. 3 displays an amplified TS-wave train initiated by the vibration-acoustic receptivity mechanism. This wave train represents the main object of the present study. These data (as well as similar ones obtained in *regimes b*, *c*, and *d*) were taken for further data processing in order to obtain the complex vibration-acoustic receptivity coefficients.

## 4. Data processing

The measured wave trains were decomposed to the normal TS-wave modes by means of the complex spatial Fourier transform. An example of the resulting spanwise wavenumber spectra is shown in Fig. 4 for *regime a*. Similarly to [1], the *initial* (i.e. at the vibrator location) spectra of the excited TS-waves were determined by an upstream extrapolation with the help of the linear stability theory. The *initial* phase spectra were obtained by a straight-line extrapolation. The results are shown in Fig. 4 as well (s = 123 mm).

The dispersion relationships $\alpha_r=\alpha_r(\beta)$ were determined by means of a linear approximation of the streamwise phase distributions for every single spanwise wavenumber. Then, the resonant

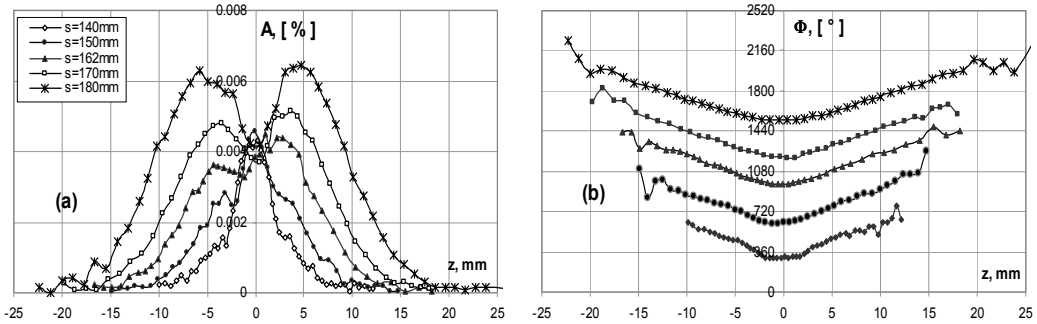


Fig. 3. Spatial development of disturbance amplitude (*a*) and phases (b) at positive combination frequency. Regime *a*.

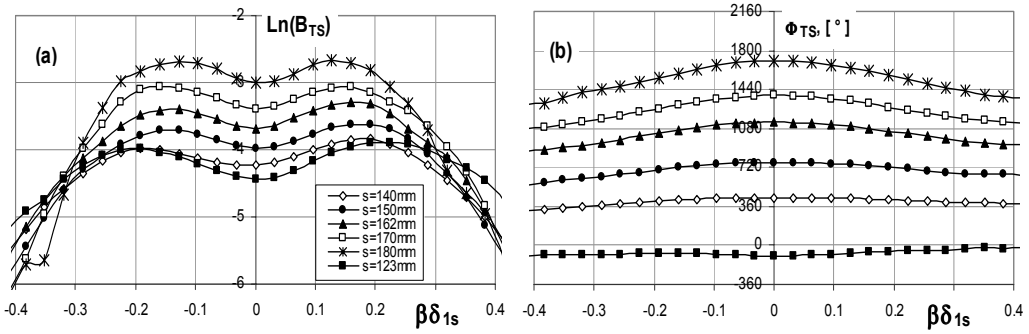


Fig. 4. Amplitude (*a*) and phase (b) spamwise-wavenumber spectra at positive combination frequency. Regime *a*.

spectral modes were selected from the 2D wavenumber spectrum of the membrane vibrations with the help of the dispersion relationships. Finally, the complex receptivity functions (amplitude and phase parts) were determined according to the definition:

$$\overline{G}_{av1,2}(\alpha_r,\beta) = G_{av1,2}(\alpha_r,\beta)\cdot e^{i\phi_{av1,2}(\alpha_r,\beta)} = \frac{\overline{B}_{inTS1,2}(\alpha_r,\beta)}{\overline{A}_{ac}\cdot\overline{A}_v(\alpha_r,\beta)}$$

where $\overline{B}_{inTS}$ is the initial spectrum of the TS-waves excited by acoustics on the vibrator, $\overline{A}_{ac}$ is the acoustic amplitude, and $\overline{A}_v$ is the spectral amplitude of the membrane vibrations (all values are complex).

## 5. Receptivity results and conclusions

The receptivity coefficients obtained for the case of scattering of acoustics due to surface vibrations are presented in the Figs. 5 and 6 versus the wave propagation angle. The data obtained for the TS-frequency $f_{TS1}$ (*regimes a-c*) are shown in Fig. 5, while those for TS-frequency $f_{TS2}$ (*regime d*) are plotted in Fig. 6. It is seen that all receptivity amplitudes presented in Fig. 5 are very close to each other, especially for 2D and moderately inclined waves, where the experimental accuracy is the highest. The obtained results do not show any dependence of the vibration-acoustic receptivity coefficients neither on the parameter of non-stationarity *K* nor on the frequencies of vibration and acoustics. A visible discrepancy for the receptivity phases can be explained, most likely, by an uncertainty of their experimental determination. The roughness-acoustic receptivity coefficients obtained in [1] for close TS-frequencies are plotted in Figs. 5 and 6 for comparison. These acoustic receptivity data determined for the roughness case ($K$ = 0, i.e. $f_v$ = 0, $f_{TS}$ = $f_{ac}$) coincide perfectly with those measured in the present experiments for scattering on surface vibrations. This result confirms the main conclusion of the present study: the vibration-acoustic receptivity (including the roughness-acoustic case) is defined by the frequency of the excited instability wave and it is independent of the frequencies of the exciting perturbations. In view of this result, the properties of the acoustic receptivity coefficients due to surface non-uniformity (stationary or non-stationary!) can be *generalised* in the following way.

It is found that free-stream acoustic perturbations interacting with surface non-uniformities excite 3D (oblique) TS-waves more effectively then 2D ones. The acoustic receptivity dependence on the wave obliqueness increases with the instability-wave frequency. The growth of this frequency leads to a relatively weak change of receptivity amplitudes for 2D waves, but

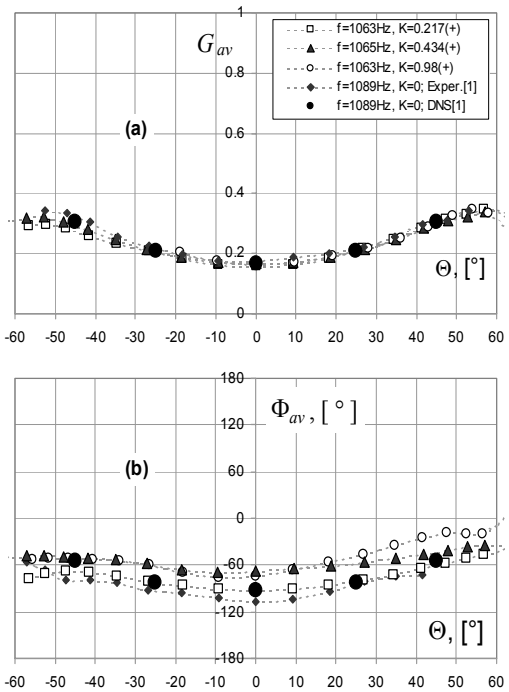


Fig. 5. Acoustic receptivity amplitudes (*a*) and phases (*b*) for frequency $f_{TS1}$. 1-3 – vibration-acoustic, *regimes a-c* respectively; 4, 5 – roughness-acoustic, experiment and DNS [1].

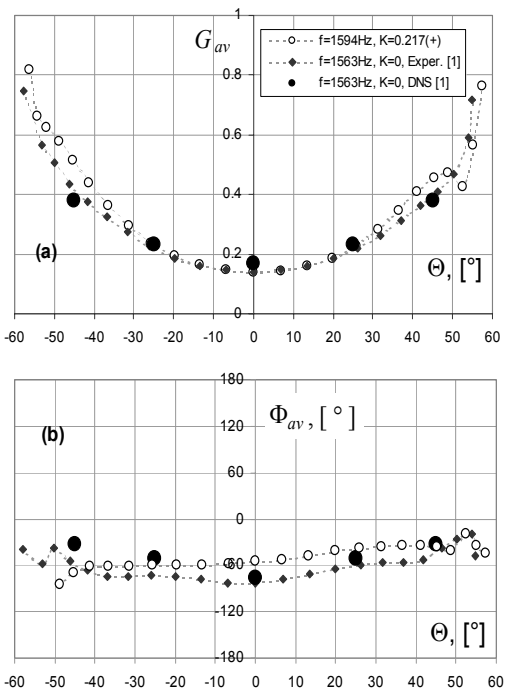


Fig. 6. Acoustic receptivity amplitudes (*a*) and phases (*b*) for frequency $f_{TS2}$. 1 – vibration-acoustic, *regime d*; 2, 3 – roughness-acoustic, experiment and DNS [1]

to their significant increase for 3D waves. The receptivity phase depends rather weakly on both the TS-wave frequency and the TS-wave obliqueness (the spanwise wavenumber). The performed set of experiments allows us to conclude, that the vibration-acoustic (or roughness-acoustic) receptivity depends solely on the frequency of the excited instability wave and it is independent of the involved vibrational and acoustic frequencies. The latter observation has an important practical meaning. In this work the situations were simulated when the external acoustic and vibrational perturbations were located in the *stable* part of the frequency spectrum and, hence, directly produced in the boundary layer only attenuating disturbances. However, by means of the vibration-acoustic receptivity mechanism, they are also able to generate instability waves in the range of *unstable* frequencies *with the same efficiency* as in case of the roughness-acoustic receptivity mechanism.

REFERENCES

1. **Würz W., Herr S., Wörner A., Rist U., Wagner S., Kachanov, Y.S.** Study of 3D wall roughness acoustic receptivity on an airfoil // Intern. Conf. on Methods of Aerophys. Research. Proc. Pt II. Novosibirsk, 2000. P. 195-200.
2. **Ivanov A.V., Kachanov Y.S., Koptsev D.B**. An experimental investigation of instability wave excitation in three-dimensional boundary layer at acoustic wave scattering on a vibrator // Thermophysics and Aeromechanics. 1997. Vol. 4, N 4. P. 359-372.